

Rectangular Dielectric Resonator Antenna with Single Band Rejection Characteristics

Mohamed Debab and Zoubir Mahdjoub

Laboratory of Electromagnetism, Photonics and Optonics (LEPO), Djillali liabes University of Sidi Bel Abbès, Sidi Bel Abbès, Algeria

<https://doi.org/10.26636/jtit.2019.124718>

Abstract—In this paper, a rectangular dielectric resonator antenna (DRA) suitable for wideband applications is presented and a band notch of WLAN (5.15–5.75) GHz is proposed. The DRA is mainly composed of a 20×20 mm rectangular dielectric resonator, coated with metal on the top surface, and a circular monopole excitation patch with an air gap insert. A coaxial line feed is used to excite the circular, planar monopole. An open-ended quarter wavelength C-shaped slot is embedded in the circular patch to create the notched band. The simulated results demonstrate that the proposed design produces an impedance bandwidth of more than 80%, ranging from 3.10 to 7.25 GHz for a reflection coefficient of less than -10 dB and with a band rejection at 5.50 GHz. Band notch characteristics, VSWR, and radiation patterns are studied using the HFSS high-frequency simulator and CST Studio software.

Keywords—band-stop function, C-shaped slot, dielectric resonator antenna (DRA), planar monopole.

1. Introduction

Dielectric resonator antennas (DRAs) are widely used due to their remarkable characteristics, such as different excitation mechanisms, small size and high permittivity. Other inherent advantages of DRAs include: low dissipation loss at high frequency, wide bandwidths and high radiation efficiency due to the absence of conductors and surface wave losses. Many investigations were focused on its bandwidth and input impedance [1]–[7]. Such parameters may easily be varied by changing the antenna's specifications, such as the dielectric constant of the resonator material, the dimensions and feed mechanisms. Special geometric configurations of DRAs may also enhance bandwidth, e.g. P-shapes, conical, cylindrical and others [8]–[10].

In the past few years, hybrid dielectric resonator antennas have received a great deal of attention due to the wideband operation that is possible without increasing antenna volume. For example, paper [11] introduced multi-segment DRAs to enhance wideband coupling between a microstrip line and a DRA, [12] proposed a hybrid-fed DRA with a stepped patch and an intermediate substrate to obtain

bandwidth between 7.5 and 12.5 GHz. In [13], a DRA was designed with an added monopole patch so that the antenna can simultaneously act as a radiator and a loading element, to produce an ultra-wide bandwidth (UWB). UWB DRAs with band stop performance have been proposed in [14], [15] and they were also designed to minimize interference between the UWB and narrowband systems, such as WiMAX and WLAN. A coplanar-fed UWB DRA with dual band-notched characteristics (WiMAX and WLAN) was created by introducing two slots in the radiation patch [16]. The notched bands are mainly implemented by adding stubs around the radiator or a feed line and etching slots onto the patch. The lengths of the etched slots or additional stubs are about a quarter wavelength or half wavelength, corresponding to the designed notch, using U-shaped [17], C-shaped [18], π -shaped [19], Y-shaped [20] or L-shaped slots [21].

In this paper, a compact wideband DRA with single band-notched characteristics (WLAN band) is presented, which uses a rectangular dielectric resonator (DR), coated with metal on the top surface, and a circular monopole excitation patch together with an air gap inserting technique. The notched frequency is realized by etching a C-shaped slot of a quarter wavelength onto the radiation patch. The tuning of the notched center frequencies is done by changing the length of the slot. The proposed antenna achieves an impedance bandwidth of 3.10 to 7.25 GHz, with a return loss being lower than -10 dB, and presents a decrement gain at approximately 5.60 GHz. The design of the antenna was first simulated using the frequency domain Ansoft high-frequency structure simulator (HFSS), and was then confirmed with the time domain CST Studio microwave simulator.

2. Antenna Design

The configuration of the proposed DRA is shown in Fig. 1. It has physical dimensions of 20×20 mm and is centrally placed above a finite ground plane with the size of 50×50 mm. The proposed DR is depicted by L_D , W_D , and $h-h_1$. The DR is designed using microwave dielectric

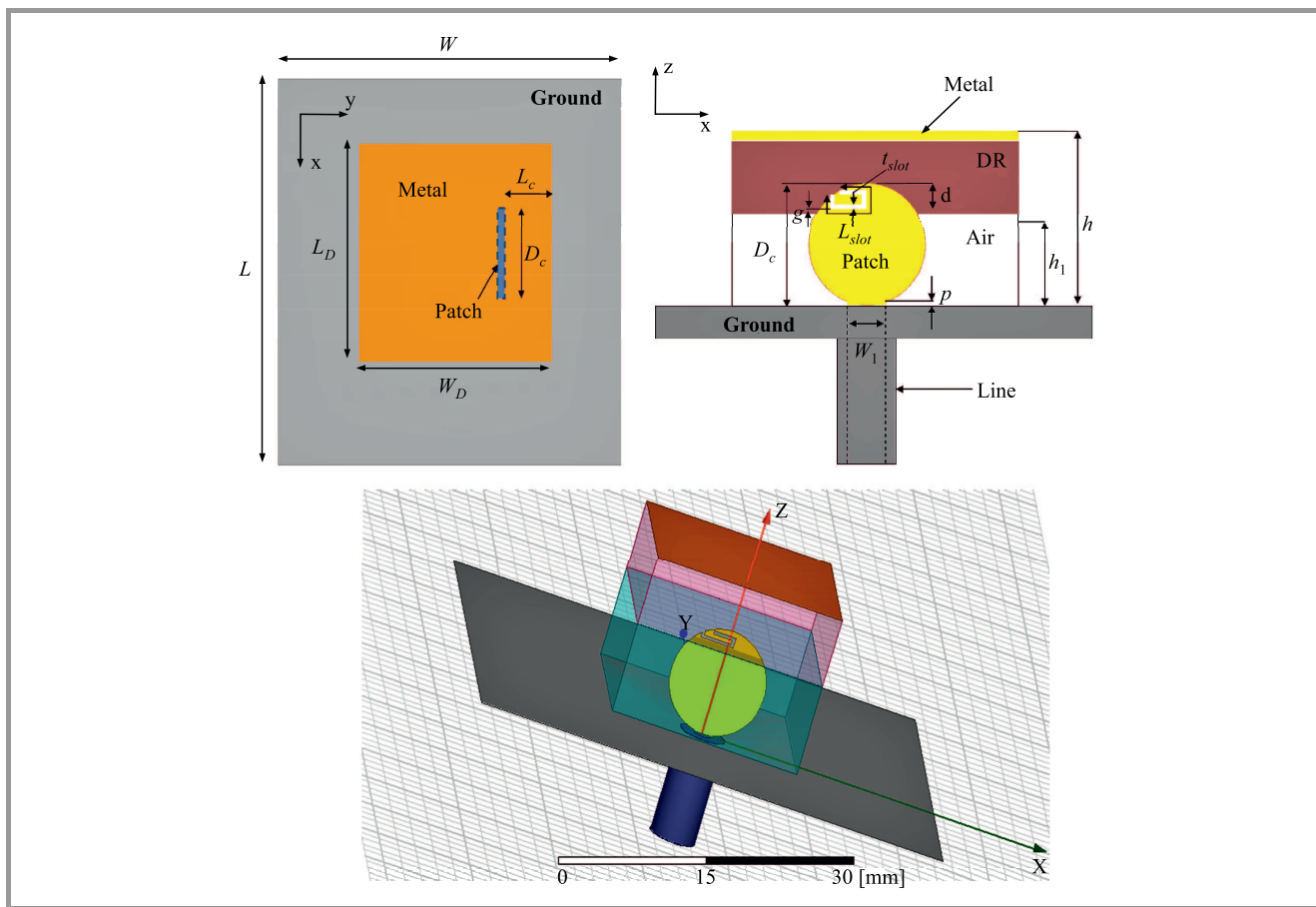


Fig. 1. Geometry of the proposed antenna.

Rogers (RO3006) material with a relative permittivity of $\epsilon_{rD} = 6.15$ and dielectric loss tangent of 0.0025.

Table 1
Optimal parameters of the proposed antenna

Parameter	Value [mm]	Parameter	Value [mm]
W	50	L_c	3
L	50	d	1.5
L_D	20	L_{slot}	7.2
W_D	20	t_{slot}	0.3
h_1	8.5	p	0.12
h	15	W_1	2
ϵ_{rD}	6.15	g	0
D_c	10		

The circle patch antenna penetrates into the DR and is connected to a 50Ω coaxial line. The thickness of the air gap inserted between the DR and the ground plane is denoted by h_1 . The exciting patch has a top width of $W_1 = 2$ mm and the width of the gap between the patch and the ground plane is $p = 0.12$ mm. A C-shaped slot of width $t_s = 0.3$ mm is etched onto the patch. The optimized parameters of the antenna are listed in Table 1.

2.1. Basic Antenna Design without C-shaped Slot

First of all, the design approach is to simulate the proposed DRA without a C-shaped slot by varying some parameters; a parametric study is then performed to see the effect on the reflection coefficients. The HFSS software was used for the parametric analysis.

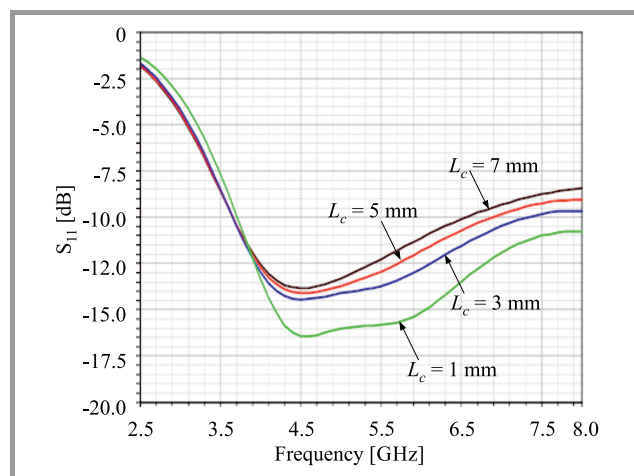


Fig. 2. Simulated S_{11} of the basic antenna (without metal coating) for different values of L_c . (For color pictures visit <https://doi.org/10.26636/jtit.2019.124718>)

Figure 2 shows the simulated S_{11} without metal coating, when the position of the patch L_c alters from 1 to 7 mm, with other parameters remaining fixed. It is clear that for S_{11} less than -10 dB, the lower edge frequency of the bandwidth is about 3.6 GHz and the height edge frequency increases. When $L_c = 3$ mm, the antenna offers a height edge frequency with the bandwidth of 7.25 GHz, and the broad impedance bandwidth of 67% for S_{11} less than -10 dB, giving the 3.60 to 7.25 GHz frequency band. The air gap between the DR and the ground plane (with the thickness h_1) plays an important role in the bandwidth enhancement. Figure 3 describes the effects of different values of h_1 . It may be seen that by introducing an air gap, the lower edge frequency decreases at 3.6 GHz when $h_1 = 8.5$ mm.

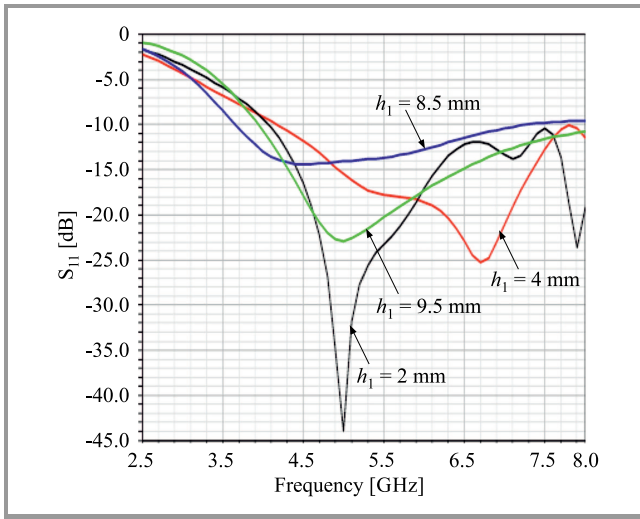


Fig. 3. Simulated S_{11} of the basic antenna (without metal coating) for different values of h_1 .

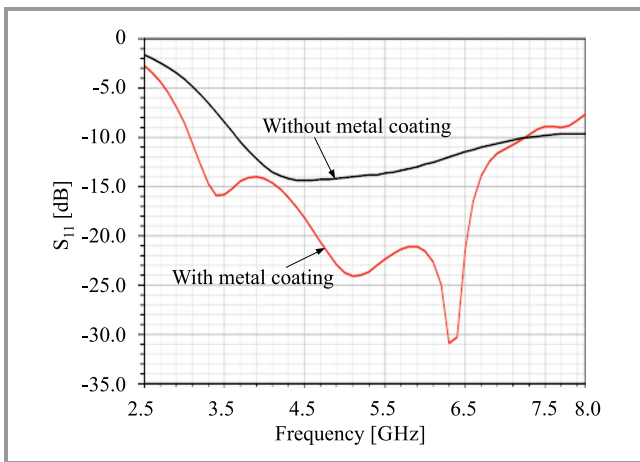


Fig. 4. Effect of the metal coating on the impedance matching characteristic.

Figure 4 illustrates the proposed antenna with and without metal coating. When the structure is not coated, the antenna works in the range of 3.60 to 7.25 GHz, with a 67% impedance bandwidth (for reflection coefficients S_{11} lower than -10 dB). When it is coated, the lower band

shifts to 3.10 GHz and the antenna has a sharp resonance dip of $S_{11} -31$ dB at 6.30 GHz with an 80% impedance bandwidth, for S_{11} lower than -10 dB, which is the highest when compared to the antenna without metal coating. The permittivity of the dielectric is much higher than that of the air. The dielectric-air interface can be approximated as a perfect magnetic conductor (PMC) boundary. The metallic foil on the dielectric resonator is treated as a perfect electrical conductor (PEC). Hence, the structure forms a cavity with PMC and PEC on different portions of the DR, filled with a high-permittivity dielectric.

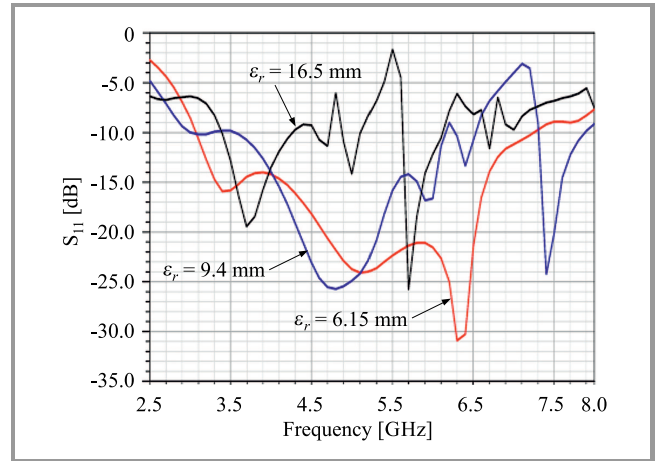


Fig. 5. Simulated reflection coefficient with different values of ϵ_{rD} with a metal coating.

It is well known that as the dielectric constant is increased, the wavelength in the DR is decreased, which results in a lower resonant frequency. Figure 5 shows the effect that DR permittivity ϵ_{rD} exerts on resonant frequencies. Increasing the permittivity leads to an increase of the Q factor, thus reducing the bandwidth of the resonant modes. Note that the resonant frequency is greatly affected by the dielectric constant. Therefore, permittivity of $\epsilon_{rD} = 6.15$ is used to design the proposed DRA.

2.2. C-shaped Slot Analysis

The central frequency of the notch band function was designed to adjust the length of the slot. The length of the slot is about a quarter of the wavelength corresponding to the resonant frequency:

$$L_{slot} \approx \frac{\lambda_g}{4} = \frac{\lambda_0}{4\sqrt{\epsilon_{eff}}} = \frac{c}{4f_{notch}\sqrt{\epsilon_{eff}}}, \quad (1)$$

$$\epsilon_{eff} = \frac{\epsilon_r + 1}{2}, \quad (2)$$

where λ_0 is the free space wavelength, f_{notch} is the central frequency of the notch band and c and ϵ_{eff} are the speed of light and the approximated effective dielectric constant, respectively.

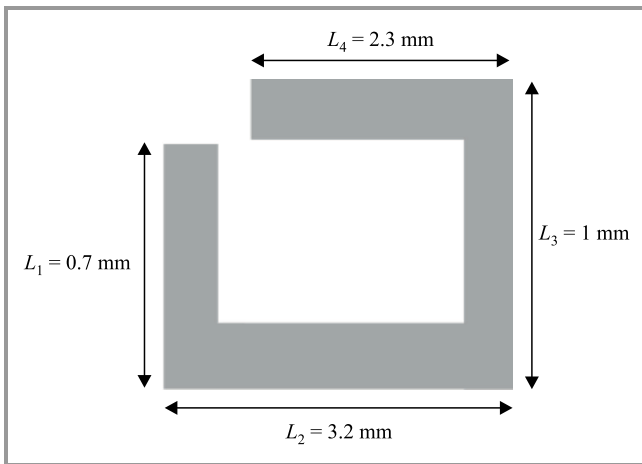


Fig. 6. C-shaped slot dimensions.

Table 2
Simulations versus theoretical predictions
for a band-notched antenna

L_1 [mm]	L_2 [mm]	L_3 [mm]	L_4 [mm]	L_{slot} [mm]	Predicted [GHz]	Simulated [GHz]
0.7	3.2	1	1.8	6.7	5.8	5.9
0.7	3.2	1	2.3	7.2	5.41	5.49
0.7	3.1	1	2.8	7.6	4.5	4.6
0.7	4.6	1	3.3	9.6	4.03	4.3

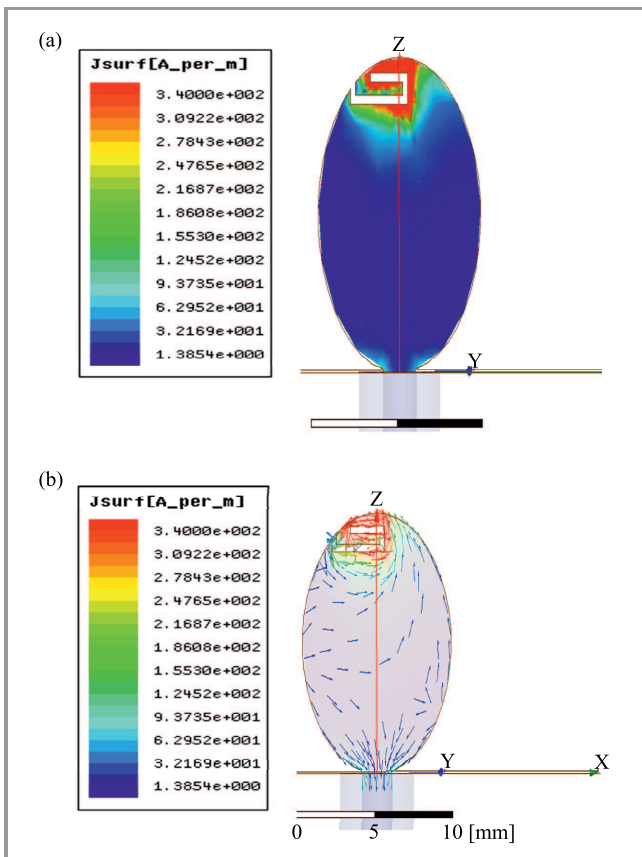


Fig. 7. Current distribution at 5.5 GHz.

The dimensions of the C-shaped slot for generating a relatively wide notch band for WLAN are shown in Fig. 6. The length of the slot can be deduced by:

$$L_{slot} \approx \frac{\lambda_g}{4} = L_1 + L_2 + L_3 + L_4 = 7.2 \text{ mm} . \quad (3)$$

When the L_s length simulation values are compared to the predictions shown in Table 2, it is found that only a few differences exist.

To understand the phenomena behind notch band performance, the simulated current distributions on WLAN band notched center frequencies were analyzed on the proposed antenna, as shown in Fig. 7. It can be observed that the current is concentrated on the edge of the slot (Fig. 7a), and that current paths around the straight slots are oriented in opposite directions (Fig. 7b). When the antenna is working at the center notched band at 5.5 GHz, the outer slot behaves as a separator.

The length of L_{slot} is varied from 6.7 to 9.6 mm. The simulated VSWR is shown in Fig. 8. It is observed that when the length of the slot is increased, the band notch shifts towards a lower frequency and the bandwidth of the notch band is increased. This is because the slot length

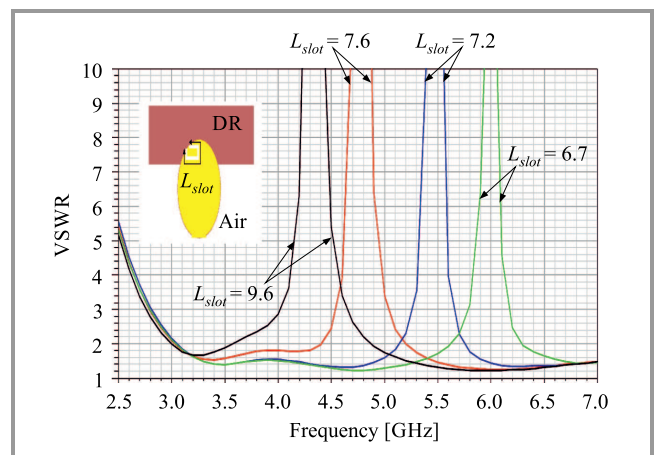


Fig. 8. VSWR characteristics of the single notch band for various L_{slot} ($h_1 = 8.5$ mm).

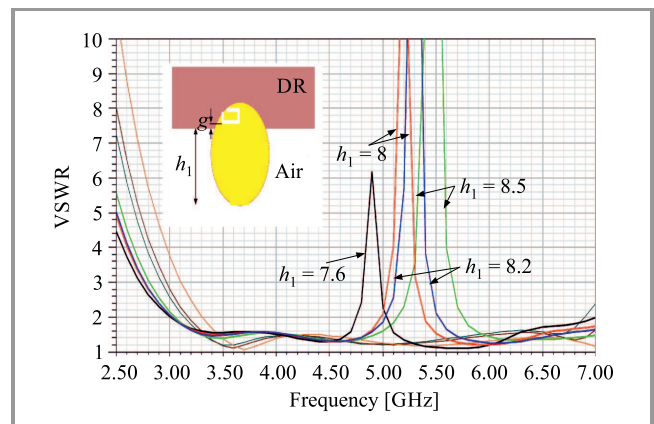


Fig. 9. VSWR characteristics of the single notch band for various h_1 ($L_{slot} = 7.2$ mm).

and notch frequency are inversely proportional to each other, as specified in Eq. (1). Interfering WLAN frequencies are within the band of 5.15 to 5.75 GHz and, hence, optimized L_{slot} is obtained at 7.2 mm for the center frequency of the WLAN band.

Gap g between the C-shaped slot and the air gap plays a crucial role in deciding the rejection band. As the gap increases from $g = 0$ ($h_1 = 8.5$ mm) to 0.9 mm ($h_1 = 7.6$ mm), the notched band shifts to the lower frequency spectrum, as shown in Fig. 9. For our requirement of rejection within the band 5.15 to 5.75 GHz, the optimized value is obtained as $h_1 = 8.5$ mm. It is observed that the notch bandwidth decreases when h_1 decreases, but with a lower peak rejection ratio.

3. Results and Discussion

The simulated VSWR plot of the proposed antenna is given in Fig. 10. It is clear that the band notch has been attained (5.15 to 5.75 GHz) and the results indicate a wide impedance bandwidth from 3.10 to 7.25 GHz. The comparison plot between the two different numerical analytical techniques, CST and HFSS, shows a similarity in verifying the performance of the antenna.

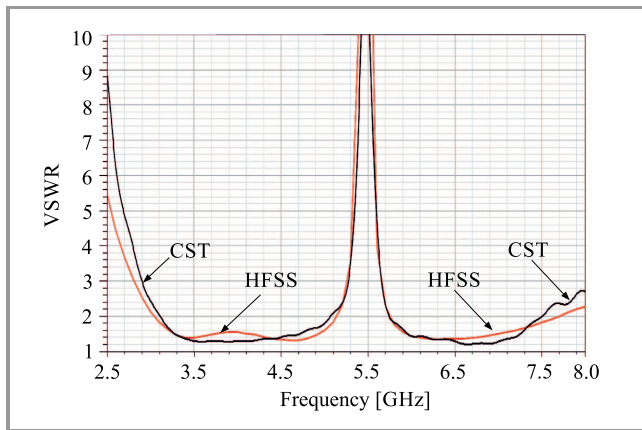


Fig. 10. Simulated VSWR using HFSS and CST software.

Figure 11 shows the simulated radiation in the E plane ($x-z$) and H plane ($x-y$) at frequencies of 3.5, 4.5, 5.5 and 6.5 GHz. The nature of H plane radiation patterns is omnidirectional, while the E plane radiation patterns are directional, which is mainly due to the effects of the metal coating. In both cases, the simulated results from the two software packages were found to be in close agreement. The antenna meets the directional requirement of UWB terminals.

The real gain comparison for the proposed DRA (with and without the C-shaped slot antenna) is shown in Fig. 12. Stable gain is observed over the entire UWB frequency range, except for band notches because the radiation at the notched band frequencies is attenuated. The real gain variation is 4.6 to 6.8 dBi. The decrease in the value of gain for the WLAN band is 9.0 dBi. As the ultra-band technol-

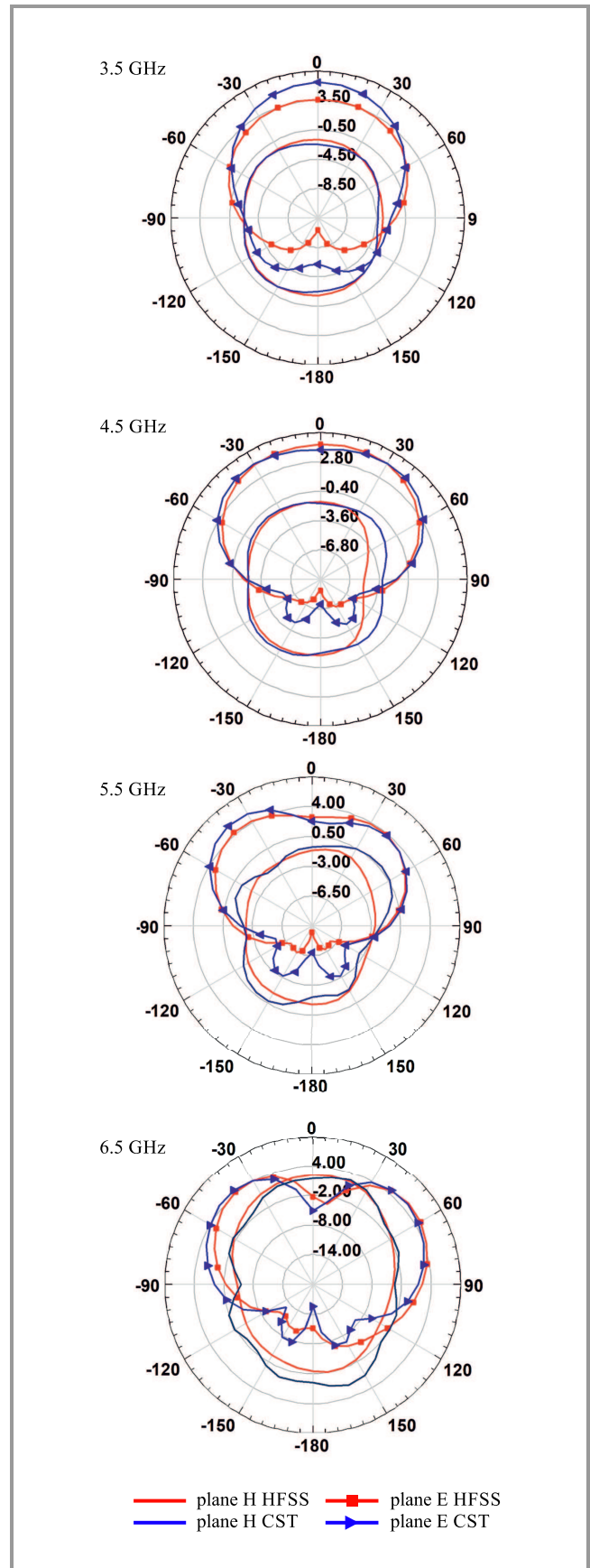


Fig. 11. HFSS and CST simulated directivity patterns in the E plane ($x-z$) and H plane ($x-y$) for the proposed antenna at 3.5, 4.5, 5.5, and 6.5 GHz.

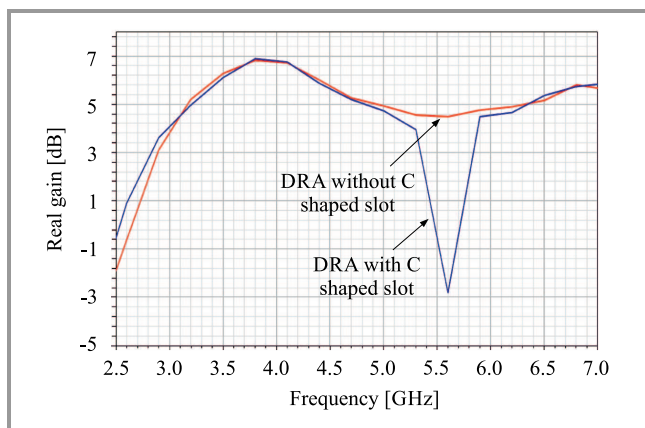


Fig. 12. Real gain versus frequency plot with and without C-shaped slot.

ogy works at a lower power level, the effect of the ultra-wideband radiation at the notched band is too weak to affect the WLAN communication system, which uses higher power levels.

4. Conclusion

The results of the simulation work conducted with the use of HFSS and CST software show that the proposed DRA provides a wide impedance bandwidth of approximately 80%, offering the range of 3.1 to 7.25 GHz, while providing one notched band operation at 5.5 GHz. This antenna is very simple in structure and has a very low overall height of $0.14\lambda_{\min}$ at its lowest operation frequency and it is able to work in the WiMAX system (3.2–3.8 GHz). This DRA is easy to fabricate and is capable of removing interference from the ultra-wideband system in the WLAN band. The impact of changes in dimensions and the position of the C-shaped slot on the band-notch characteristics of the proposed antenna was analyzed as well. It was observed that the notched band can be adjusted by changing the thickness of DRA. The air gap, the metal coating on the top and the position of the patch are important for improving DRA bandwidth. Furthermore, the proposed antenna demonstrated a good omnidirectional radiation pattern, an acceptable gain in operating frequencies and may be a good candidate for wireless applications.

References

- [1] S. Keyrouz, and D. Caratelli, "Dielectric resonator antennas: basic concepts, design guidelines", *Int. J. on Antennas and Propag.*, vol. 2016, Article ID 6075680 (doi: 10.1155/2016/6075680).
- [2] K. M. Luk and K. W. Leung, *Dielectric Resonator Antennas*. Hertfordshire, UK: Research Studies Press, 2003 (ISBN 9780863802638).
- [3] R. N. Simons and R. Q. Lee, "Effect of parasitic dielectric resonator on CPW aperture-coupled dielectric resonator antenna", *IEE Proc. H, (Microw. Antennas and Propag.)*, vol. 140, no. 5, pp. 336–338, 1993 (doi: 10.1049/ip-h-2.1993.0052).
- [4] M. S. Al Salameh, Y. M. M. Antar, and G. Seguin, "Coplanar-waveguide-fed slot-coupled rectangular dielectric resonator antenna", *IEEE Trans. on Antennas and Propag.*, vol. 50, no. 10, pp. 1415–1419, 2002 (doi: 10.1109/TAP.2002.802097).
- [5] T. H. Chang and J. F. Kiang, "Broadband dielectric resonator antenna with metal coating", *IEEE Trans. on Antennas and Propagation*, vol. 55, no. 5, pp. 1254–1259, 2007 (doi: 10.1109/TAP.2007.895582).
- [6] Q. Rao, T. A. Denidni, A. R. Sebak, and R. H. Johnston, "Compact independent dual-band hybrid resonator antenna with multi-functional beams", *IEEE Microw. and Wirel. Compon. Lett.*, vol. 5, pp. 239–242, 2006 (doi: 10.1109/LAWP.2006.875886).
- [7] K. W. Leung and K. K. So, "Frequency-tunable designs of the linearly and circularly polarized dielectric resonator antenna using a parasitic slot", *IEEE Trans. on Antennas and Propag.*, vol. 53, no. 1, pp. 572–578, 2005 (doi: 10.1109/TAP.2004.838762).
- [8] A. A. Kishk, Y. Yin, and A. W. Glisson, "Conical dielectric resonator antennas for wide-band applications", *IEEE Trans. on Antennas and Propag.*, vol. 50, no. 4, pp. 469–474, 2002 (doi: 10.1109/TAP.2002.1003382).
- [9] B. N. Taralkar and A. R. Wadhekar, "Fractal dielectric resonator antenna for wideband applications", *Adv. Res. in Elec. and Electron. Engin.*, vol. 2, no. 5, pp. 1–3, 2015 [Online]. Available: https://www.krishisanskriti.org/vol_image/24Sep201509093401%20Bajrang%20N%20%20Taralkar.pdf
- [10] Z. Chen and H. Wong, "Wideband glass and liquid cylindrical dielectric resonator antenna for pattern reconfigurable design", *IEEE Trans. on Antennas and Propag.*, vol. 65, no. 5, pp. 2157–2164, 2017 (doi: 10.1109/TAP.2017.2676767).
- [11] A. Petosa, N. Simons, R. Siushansian, A. Ittipiboon, and M. Cuhaci, "Design and analysis of multi segment dielectric resonator antennas", *IEEE Trans. on Antennas and Propag.*, vol. 48, pp. 738–742, 2000 (doi: 10.1109/8.855492).
- [12] Y. Coulibaly, T. A. Denidni, and H. Boutayeb, "Broadband microstrip fed dielectric resonator antenna for x-band applications", *IEEE Antennas and Wirel. Propag. Lett.*, vol. 7, pp. 341–345, 2008 (doi: 10.1109/LAWP.2008.921326).
- [13] M. Lapiere, Y. M. M. Antar, A. Ittipiboon, and A. Petosa, "Ultra wideband monopole dielectric resonator antenna", *IEEE Microw. and Wirel. Compon. Lett.*, vol. 15, no. 1, pp.7–9, 2005 (doi: 10.1109/LMWC.2004.840952).
- [14] M. Abedian, S. K. A. Rahim, Sh. Danesh, M. Khalily, and S. M. Noghabaei, "Ultrawideband dielectric resonator antenna with WLAN band rejection at 5.8 GHz", *IEEE Microw. and Wirel. Compon. Lett.*, vol. 12, pp. 1523–1526, 2013 (doi: 10.1109/LAWP.2013.2291271).
- [15] Y. F. Wang, T. A. Denidni, Q. S. Zeng, and G. Wei, "Band-notched UWB rectangular dielectric resonator antenna" *Electron. Lett.*, vol. 50, no. 7, pp. 483–484, 2014 (doi: 10.1049/el.2014.0188).
- [16] T. A. Denidni and Z. Weng, "Hybrid ultrawideband dielectric resonator antenna and band-notched designs", *IET Microw. Antennas Propag.*, vol. 5, no. 4, pp. 450–458, 2011 (doi: 10.1049/iet-map.2009.0425).
- [17] Y. J. Cho, K. H. Kim, D. H. Choi, S. S. Lee, and S. Park, "A miniature UWB planar monopole antenna with 5GHz band rejection filter and the time domain characteristics", *IEEE Trans. on Antennas and Propag.*, vol. 54, no. 5, pp. 1453–1460, 2006 (doi: 10.1109/TAP.2006.874354).
- [18] A. Syed and R. W. Aldhaheeri, "A very compact and low profile UWB planar antenna with WLAN band rejection", *The Scient. World J.*, vol. 2016 (doi: 10.1155/2016/3560938).
- [19] Y. Li, W. Li, and Q. Ye, "A reconfigurable triple-notch-band antenna integrated with defected microstrip structure band stop filter for ultra wideband cognitive radio applications", *Int. J. of Antennas and Propag.*, vol. 2013, no. 7, Article ID 472645 (doi: 10.1155/2013/472645).
- [20] W. C. Liu and C. F. Hsu, "Dual-band CPW-fed Y-shaped monopole antenna for PCS/WLAN application", *Electron. Lett.*, vol. 41, no. 17, pp. 390–391, 2005 (doi: 10.1049/el:20057887).

- [21] N. D. Trang, D. H. Lee, and H. C. Park, "Compact printed CPW-fed monopole ultra-wideband antenna with triple subband notched characteristics", *Electron. Lett.*, vol. 46, no. 17, pp. 1177-1179, 2010 (doi: 10.1049/el.2010.1140).



Mohamed Debab received his B.Sc. degree in Electronics from the Electronics Institute of the University of Djillali Liabes, Sidi Bel Abbes, Algeria, in 1998. Then he received an M.Sc. from the Department of Electronics, University of Djillali Liabes, Sidi Bel Abbes, Algeria, 2005. Currently, he is working as an Assistant Profes-

sor at the Department of Electronics, University of Hassiba Ben Bouali Chlef Algeria. His research interests focus on design and analysis of coplanar and dielectric antennas.

 <https://orcid.org/0000-0002-1779-0323>

E-mail: debab_telecoms2005@hotmail.fr

Laboratory of Electromagnetism, Photonics and Optronics (LEPO)

Djillali liabes University of Sidi Bel Abbès
22000 Sidi Bel Abbès, Algeria



Zoubir Mahdjoub received his B.Sc. degree in Electronics from the Electronics Institute of USTO of Oran, Algeria, in 1982, a Diploma of Advanced Studies, from the National Polytechnic Institute of Grenoble, France, in 1983, and a Ph.D. degree from the University of Claude Bernard de Lyon I, France, in 1987. Between 1988

and 1991, he was the President of the Scientific Council of the Electronics Institute, University of Djillali Liabes, Sidi Bel Abbes, Algeria. Since 1988, he has been involved in conducting research on microwaves, telecommunications and photonics. Between 1998 and 2006, he was the head of the Electronics Department, University of Djillali Liabes. He is now a full professor and a vice dean for post-graduation programs at the Electrical Engineering Faculty of the same University.

E-mail: mahdjoubz@yahoo.com

Laboratory of Electromagnetism, Photonics and Optronics (LEPO)

Djillali liabes University of Sidi Bel Abbès
22000 Sidi Bel Abbès, Algeria